LAWRENCE
LIVERMORE
NATIONAL
LABORATORY

LLNL-PROC-556936

Comparison of ELM heat loads in snowflake and standard divertors

T. D. Rognlien, R. H. Cohen, D. D. Ryutov, M. V. Umansky

May 9, 2012

International Conference on Plasma Surface Interactions
Aachen, Germany
May 21, 2012 through May 25, 2012

Disclaimer

LLNL-PROC-556936

Comparison of ELM heat loads in snowflake and standard divertors

T.D. Rognlien*, R.H. Cohen, D.D. Ryutov, and M.V. Umansky

Lawrence Livermore National Laboratory, 7000 East Ave, Livermore, CA 94551 USA

Abstract

An analysis is given of the impact of the tokamak divertor magnetic structure on the temporal and spatial divertor heat flux from edge localized modes (ELMs). Two configurations are studied: the standard divertor where the poloidal magnetic field (B_p) varies linearly with distance (r) from the magnetic null and the snowflake where B_p varies quadratrically with r. Both one- and two-dimensional models are used to analyze the effect of the longer magnetic field length between the midplane and the divertor plate for the snowflake that causes a temporal dilation of the ELM divertor heat flux. A second effect discussed is the appearance of a broad region near the null point where the poloidal plasma beta can substantially exceed unity, especially for the snowflake configuration during the ELM; such a condition is likely to drive additional radial ELM transport.

PACS: 52.55.Rk, 52.30.Ex, 52.65.Kj, 52.55.Fa

PSI-20 keywords: Edge modelling, ELM control, Divertor, Divertor modeling, UEDGE

**Corresponding author address:* LLNL, P.O. Box 808, L-637, Livermore, CA 94551 USA

**Corresponding author E-mail:* trognlien@llnl.gov

**Presenting author:* I. Joseph

1. Introduction

Material surfaces surrounding fusion devices must accommodate the large steady-state plasma heat exhaust that is localized spatially, typically near the intersection of the magnetic separatrix and the divertor plate. In addition, an abrupt release of plasma with very high heat flux of limited duration can occur from edge-localized modes (ELMs), which produces a limitation on the acceptable ELM size for future devices including ITER [1]. The ELM dominantly flows along magnetic fields lines to the divertor plates in a relatively short time (~ 0.1-1 millisecs). This paper thus analyzes the temporal and spatial characteristics of the ELM divertor heat flux, first showing that the longer magnetic field length in the snowflake divertor (SFD) configuration [2] can have substantially smaller peak heat flux rise than a standard X-point divertor (STD) for the same midplane ELM characteristics. Secondly, it is shown that the poloidal plasma beta (β_p) is larger than unity over an extended region near the magnetic null for the SFD and argued that this condition indicates strong plasma convection with radial spreading of the ELM energy [3]. (In SI units, $\beta_p=2\mu_0 P/B_p^2$ for plasma pressure P, poloidal magnetic field B_p, and vaccum permeability μ_0.) There are experimental results from the TCV device showing that the SFD has significant impact on ELM characteristics [4], including recent observations of reduced peak heat flux [5].

The potential to seriously damage the divertor material depends on both the time over which the energy is deposited and the radial width of the energy pulse. The first effect depends on the increased length, L, of the magnetic field line between the midplane and divertor plate. For a simple 0D model, the surface temperature rise scales approximately as $E_{elm}/\tau_d^{1/2}$, where E_{elm} is

the total ELM energy deposited, and τ_d is the deposition time on the surface [1]. Because of the increased L for the SFD, τ_d, and the temperature rise will be smaller. Furthermore, for larger τ_d, the anomalous radial transport will cause more radial spreading of the ELM energy that lowers local plate heating. An example of the variation of L with distance from the separatrix for SFD and STD is shown in Fig. 1 (from Ref. [6], Fig. 8).

The second heat-flux reduction effect considered is the extent of the $\beta_p > 1$ region near the magnetic null point. As discussed in more detail in Ref. [3], the standard plasma equilibrium maintained by both poloidal and toroidal magnetic fields is not viable when the plasma pressure substantially exceeds the poloidal magnetic pressure; the toroidal current proportional to B_p can become too small to maintain the equilibrium and local instabilities can also arise. The SFD yields much larger β_p than the STD because of its extended region of low B_p, and these values are further enhance during the ELM owing to a larger plasma pressure.

2. Approach and models

The plasma and neutrals are described by the UEDGE fluid transport code operated in both 1D and 2D modes, which includes time-dependent equations for the spatial variation of plasma and neutral particle densities (n_i and n_g), parallel (along the total magnetic field, $\boldsymbol{B}$) velocities ($v_{||i}$ and $v_{||g}$), electron temperature (T_e), and combined ion/neutral temperature (T_i) [7]. The justification of such a fluid model for modeling the ELM temporal response is illustrated by the results in Ref. [8]. For the one-dimensional (1D) model used here, the variation along $\boldsymbol{B}$ is simulated using flux-limited classical collisional transport coefficients, and ion/electron energy exchange is included. Particle recycling of ion/electron pairs into neutrals occurs at bounding

material surfaces with the recycling yield coefficient of $R_p = 0.99$, and energy is absorbed at the boundaries. Multi-step ionization and recombination processes are included. The ELM is simulated by particle and energy sources switched on for a short time (typically 200 μs) and localized at one end of the domain having symmetry boundary conditions. The second end corresponds to the divertor plate.

For the case of two spatial dimensions (2D), the full standard and snowflake MHD equilibria correspond to conceptual double-null device FDF [9] are used for the computational domain. The cross-field velocities are obtained from an assumed anomalous radial diffusion coefficients of 0.33 m^2/s for density and 0.5 m^2/s for $v_{||i}$, T_e, and T_i. Other processes are as for the 1D model, with the pulsed ELM particle and energy source located very near the midplane. The 1D analysis focuses on the effect of increased connection length L. The 2D model allows evaluation of the effect of L being a function of distance from the separatrix (see Fig. 1), radial transport, and an assessment of the size of the $\beta_p > 1$ region near the magnetic null point.

3. Results

The results of the 1D model is shown in Fig. 2 for a range of lengths L that can be expected near the separatrix for the snowflake configuration. The ELM source has a width of 1 m along $\boldsymbol{B}$ for all cases. The divertor heat flux is composed of ion and electron particles energy, potential energy released by plate recombination, and radiation (here only from hydrogen). On the plasma side of the plate sheath, the electron energy deposition dominates earlier in time, but at the plate itself, the sheath acceleration of ions and retarding of electrons results in the ion channel always being the dominant energy component. The right-hand panel of Fig. 2 shows the time-integrated

energy deposited. The time for ½ of the energy to arrive begins to scale linearly L for large values. For a diffusive process (thermal conduction), a scaling with L^2 is expected, but these cases quickly reach the flux (or sheath)-limited regime for electron conduction, and both it and convective transport scale as L as shown, with a transport time of $\tau_{||} \sim L/[(T_e+T_i)/m_i]^{1/2}$.

The 2D results use the flux-surface mesh obtained from the double-null MHD equilibrium as shown in Fig. 3; note the larger flux-expansion near the magnetic null point for this snowflake-plus (SFDP) configuration [1]. The SFDP has two nearby magnetic nulls, only one of which is shown in Fig. 3; it is topologically more stable that the exact snowflake [1] and is more convenient to study numerically. The ELM is simulated by a particle and energy sources localized at the outer midplane, and the base case considers a modest ELM of 40 kJ and 1.3×10^{20} particles injected over a 200 μs period. The heat-flux components for each divertor configuration are shown in Fig. 4 at 200 μs on the divertor surface and include the ion acceleration and electron retardation through the plasma sheath. The plate recombination component is the atomic binding energy released upon recombination of ion/electron pairs in the plate. The SFDP configuration clearly has a broader footprint – by a factor of ~3 with the peak value being 0.40 that of the STD. Part of the increase in the SFDP heat-flux width is due to the magnetic flux expansion at the plate, which a comparison mapped to the midplane removes. This comparison of heat-flux mapped to the outer midplane is shown in Fig. 4, together with the radial width of the ELM source, showing that the SFDP still as about twice the width and 0.67 the peak value of the STD. The plate comparisons are most relevant to assessing damage to material.

The assessment of β_p is shown in Fig. 5, comparing the SFDP before and during the ELM with the STD during the ELM. The region inside the white-dashed line has $\beta_p > 1$. Because of the smaller poloidal field for the SFDP, it has a large area with $\beta_p > 1$, with the during-ELM values about a factor of 2 above the pre-ELM values. In contrast, the STD barely achieves $\beta_p = 1$ even during this modest 40 kJ ELM. From Ref. [3], the relevance of large $\beta_p > 1$ is that magnetic-curvature-driven flute instabilities are no longer stabilized by B_p. The resulting flute mode growth rate is then

$$\Gamma \sim [(\partial P/\partial r)/(m_i n_i R)]^{1/2}, \quad (1)$$

where m_i is the ion mass, and R is the major radius. Comparing the anticipated turbulence eddy turn-over time τ_e to the parallel convection time of the ELM, gives the scaling [3]

$$\tau_{\|}/\tau_e \sim (B_T/B_{pm})(a^2/R\Delta)^{1/2}, \quad (2)$$

where B_T, B_{pm}, and Δ are the toroidal and poloidal magnetic fields and the ELM width, all at the midplane, respectively, and a is the minor radius. For case studied here, $\tau_{\|}/\tau_e \sim 15$, indicating strong radial spreading during the parallel transit time when $\beta_p >> 1$. In addition, the SFD has two extra divertor legs (nearby, but not shown if Fig. 3), and strong null-region transport can cause further reduction in the local ELM heat flux by power sharing with the other legs [3, 5].

4. Summary

The results of 1D and 2D simulations show that the peak divertor heat flux from an ELM can be substantially smaller for the snowflake divertor compared to the standard divertor. The increased connection length for the SDF causes a temporal dilation of the energy pulse, lessening

the surface heating and allowing more time for radial transport of ELM energy. In addition, the SDF shows a large region around the null point where $\beta_p > 1$, especially during the ELM, indicating that flute instabilities may further spread the ELM energy across field lines. These results provide a possible explanation for the lower SDF ELM heat flux observed in NSTX and TCV [5].

Acknowledgements The authors are grateful to V. Soukhanovskii and H. Reimerdes, and their respective NSTX and TCV team members for helpful discussions. This work was performed for U.S. DoE by LLNL under Contract DE-AC52- 07NA27344.

References

[1] A. Loarte, G. Saibene, R. Sartori *et al.*, Phys. Plasmas **11** (2004) 2668.

[2] D.D. Ryutov, Phys. Plasma **14** (2007) 064502.

[3] D.D. Ryutov, R.H. Cohen, T.D. Rognlien, M.V. Umanksy, Contrib. Plasma Phys. **52** (2012) 539.

[4] F. Piras, S. Coda, B.P. Duval *et al*., Phys. Rev. Lett. **105** (2010) 155003.

[5] V.A. Soukhanovskii, H. Reimerdes *et al.,* invited paper, this conference.

[6] D.D. Ryutov, R.H. Cohen, T.D. Rognlien, M.V. Umansky, Phys. Plasmas **15** (2008) 092501.

[7] T.D. Rognlien and M.E. Rensink, Fusion Eng. Design **60** (2002) 497; and references therein.

[8] E. Havlıckova, W. Fundamenski, D. Tskhakaya *et al*., Plasma Phys. Contr. Fusion **54** (2012) 045002.

[9] A.M. Garofalo, V.S. Chan, R.D. Stambaugh *et al.* IEEE Trans. Plasma Sci. **38** (2010) 461.

Figure captions

1. Comparison of normalized magnetic field line lengths for snowflake (heavy line) and standard divertor (light line) versus normalized distance from the magnetic separatrix; from Ref. [6], Fig. 8, where the normalization constants are defined.

2. Divertor heat flux versus time with the 1D model for various magnetic field-line lengths and the time-integrated fraction of the ELM pulse energy reaching the divertor plate.

3. Magnetic flux-surface computational mesh for the standard and snowflake-plus divertors.

4. Heat-flux profiles in the 2D model at 200 μs for the standard and snowflake-plus divertors.

5. Poloidal plasma beta (β_p) for snowflake and standard divertor cases at times indicated. The dotted white line corresponds to $\beta_p = 1$ contour.

Figure 1

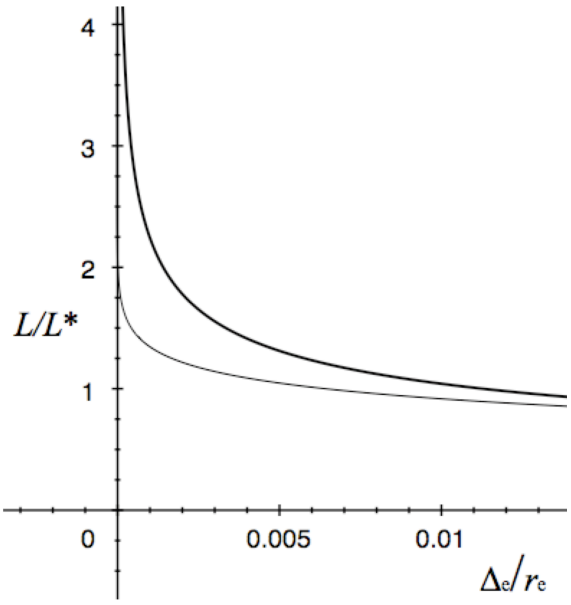

Figure 2

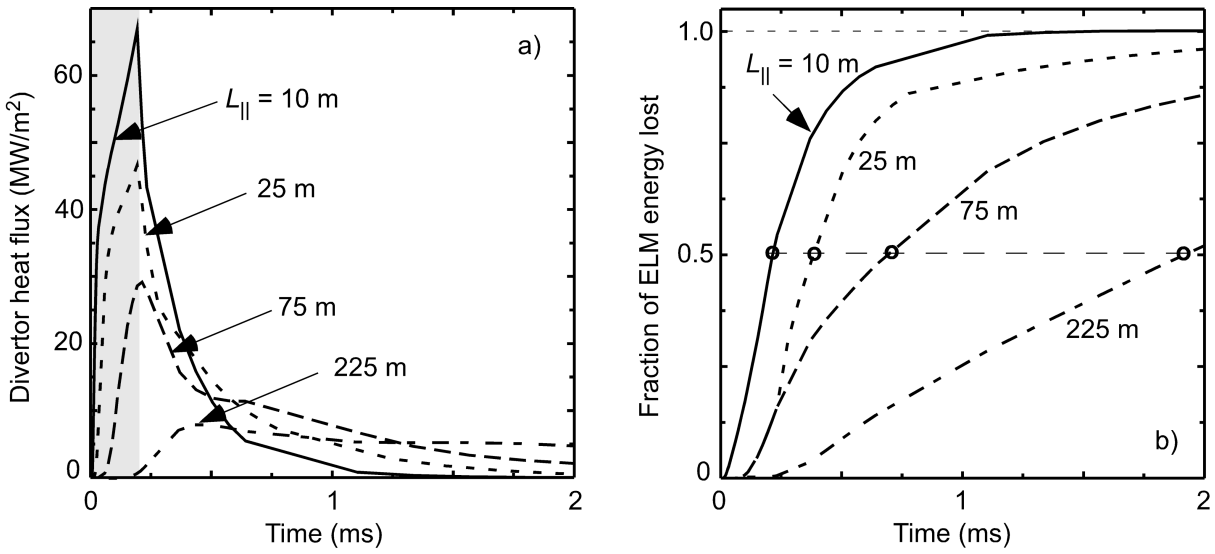
a)
Divertor heat flux (MW/m^2)
60
40
20
0
0
1
2
Time (ms)
$L_{||}$ = 10 m
25 m
75 m
225 m
b)
Fraction of ELM energy lost
1.0
0.5
0
0
1
2
Time (ms)
$L_{||}$ = 10 m
25 m
75 m
225 m

Figure 3

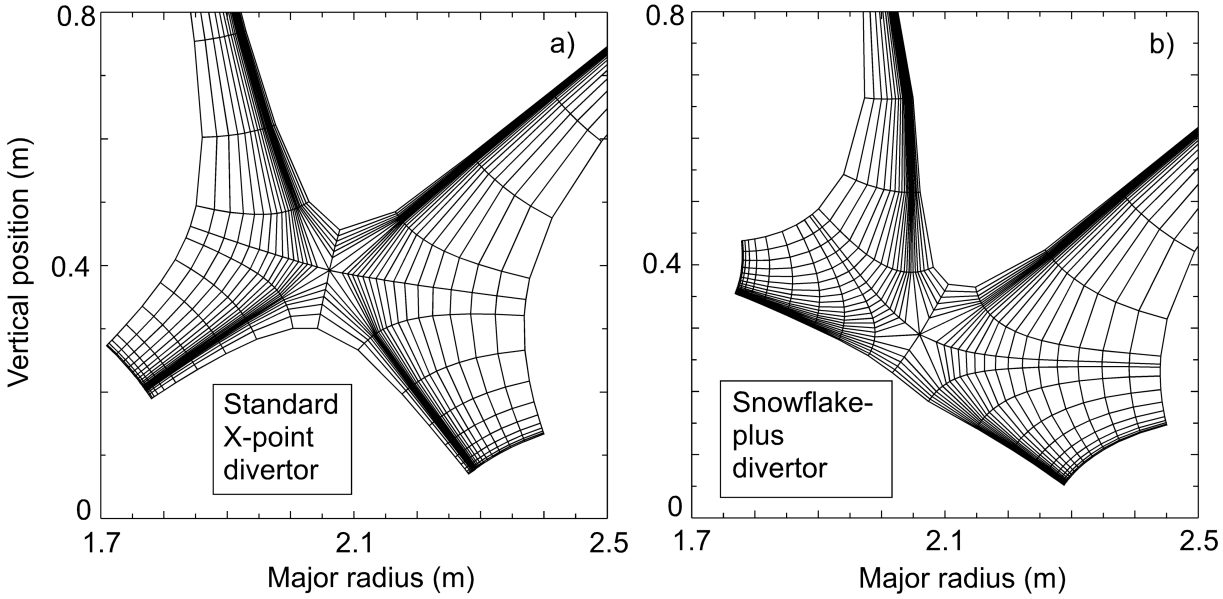
0.8
0.4
0
Vertical position (m)
a)
Standard
X-point
divertor
1.7
2.1
2.5
Major radius (m)
0.8
0.4
0
b)
Snowflake-
plus
divertor
1.7
2.1
2.5
Major radius (m)

Figure 4

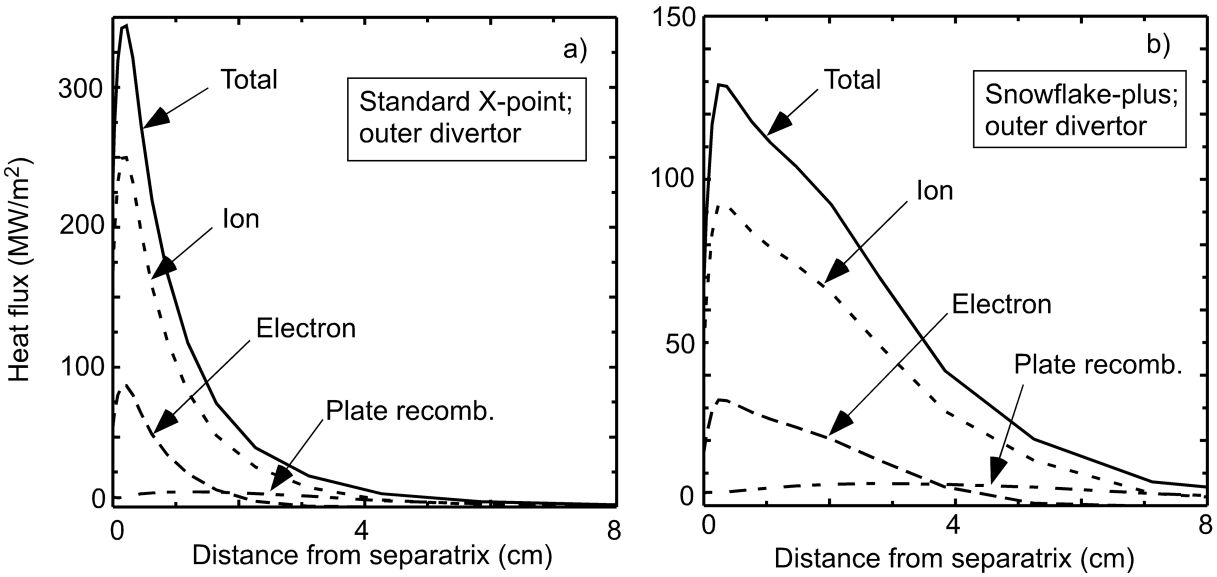
a)
Standard X-point;
outer divertor
Total
Ion
Electron
Plate recomb.
Heat flux (MW/m2)
300
200
100
0
0
4
8
Distance from separatrix (cm)
b)
Snowflake-plus;
outer divertor
Total
Ion
Electron
Plate recomb.
150
100
50
0
0
4
8
Distance from separatrix (cm)

Figure 5

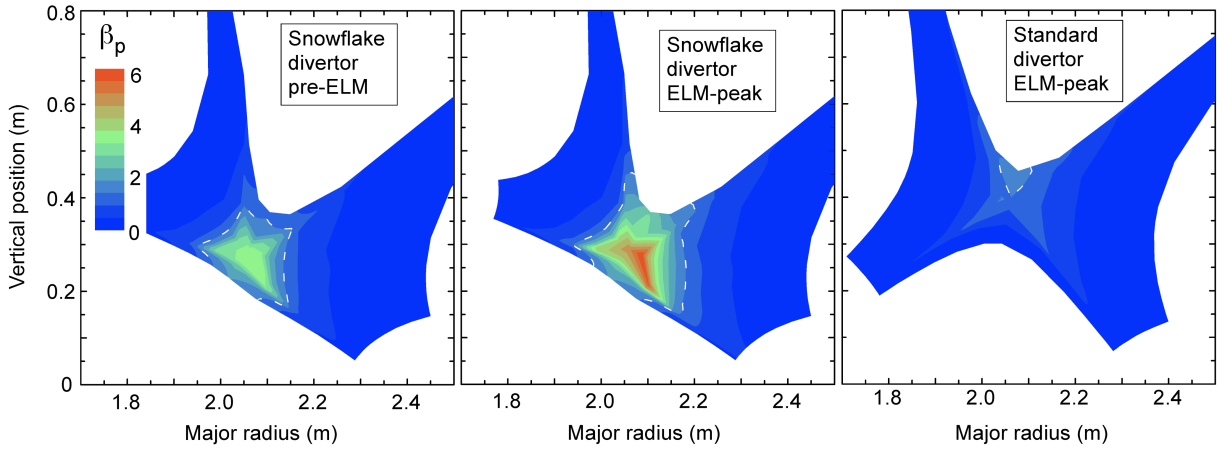
β_p
6
4
2
0
Snowflake divertor pre-ELM
Snowflake divertor ELM-peak
Standard divertor ELM-peak
Vertical position (m)
0.8
0.6
0.4
0.2
0
1.8
2.0
2.2
2.4
Major radius (m)